ABSTRACT

Title of Thesis: DECODING REPETITIVE FINGER MOVEMENTS WITH BRAIN SIGNALS ACQUIRED VIA NONINVASIVE ELECTROENCEPHALOGRAPHY

Andrew Young Paek, Master of Science, 2011

Thesis directed by: Associate Professor Jose Luis Contreras-Vidal
Department of Kinesiology, Graduate Program in Neuroscience and Cognitive Science, Fischell Department of Bioengineering

We investigated how well finger movements can be decoded from electroencephalography (EEG) signals. 18 hand joint angles were measured simultaneously with 64-channel EEG while subjects performed a repetitive finger tapping task. A linear decoder with memory was used to predict continuous index finger angular velocities from EEG signals. A genetic algorithm was used to select EEG channels across temporal lags between the EEG and kinematics recordings, which optimized decoding accuracies. To evaluate the accuracy of the decoder, the Pearson's correlation coefficient (r) between the observed and predicted trajectories was calculated in a 10-fold cross-validation scheme. Our results (median r = .403, maximum r = .704), compare favorably with previous studies that used electrocorticography (ECoG) to decode finger movements. The decoder used in this study can be used for future brain machine interfaces, where individuals can control peripheral devices through EEG signals.

DECODING REPETITIVE FINGER MOVEMENTS WITH BRAIN SIGNALS ACQUIRED VIA NONINVASIVE ELECTROENCEPHALOGRAPHY

by

Andrew Young Paek

Thesis submitted to the Faculty of the Graduate School of the
University of Maryland, College Park in partial fulfillment
of the requirements for the degree of
Master of Science
2011

Advisory Committee:

Associate Professor José Luis Contreras-Vidal, Chair
Assistant Professor Sameer Shah
Professor Yang Tao

Acknowledgements

I would like to thank my advisor José (Pepe) L. Contreras-Vidal for his mentorship behind this research, Kimberly Kontson for her assistance in obtaining the data, Harshavardhan Agashe for his contributions and advice to the project, Alessandro Presacco and Shikha Prashad for their advice, and the participants who volunteered for this study.

Part of this work was previously presented in the 15th International Graphonomics Society Conference 2011 in Live Aqua Cancun, Mexico, June 12-15, 2011. The paper received a Best Paper Award for a student presentation.

Table of Contents

List of Tables

List of Figures

List of Abbreviations

Electroencephalography (EEG)
Electrocorticography (ECoG)
Even-Related De-synchronizations (ERD)
Even-Related Synchronizations (ERS)
Functional Magnetic Resonance Imaging (fMRI)
Local Motor Potential (LMP)
Local field Potential (LFP)
Metacarpal-phalangeal (MCP)
Power Spectral Density (PSD)
Range of Motion (ROM)

1. Introduction

1.1. State of the Art

Understanding how the human brain controls hand movements presents an interest to researchers in neuroscience, engineering, and robotics because of the hand's usefulness and its inherent complexity in its multiple degrees of freedom (Schieber & Santello, 2004). Such knowledge could be used to develop control algorithms to command hand based prosthetic devices, which would be of great benefit to individuals with motor deficiencies such as paralysis or limb amputation.

Neuroimaging studies such as functional magnetic resonance imaging (fMRI) have suggested that the movement of each finger is represented in separate somatotopic, but largely overlapping, areas of the primary motor cortex and the supplementary motor areas of the human brain (Beisteiner et al., 2001; Indovina & Sanes, 2001). Moreover, another fMRI study suggested that the supplementary motor area is activated before the primary motor cortex during finger movements (Wildgruber, Erb, Klose, & Grodd, 1997). Other fMRI studies have found that a wide neural network that incorporates the prefrontal cortex and areas in the parietal lobe of the brain are responsible for planning different grasping and finger motions (Gallivan, McLean, Valyear, Pettypiece, & Culham, 2011; Toni, Schluter, Josephs, Friston, & Passingham, 1999). While these studies give a strong sense of which brain areas are active during hand movements, the temporal relationship between neural activity and hand movements are difficult to understand from these studies. Such fMRI studies usually measure the hemodynamic response in the brain, which is suspected to be delayed with respect to neural activations (Beisteiner et al., 2001; Wildgruber et al., 1997). Other neuroimaging studies which use

modalities with higher temporal resolutions complements the results found in these fMRI studies.

Electroencephalography (EEG) studies have also investigated how hand movements change brain activity. Event-related desynchronizations (ERDs), which are decreases in power in the brain's alpha (8-12 Hz) rhythms, were found to occur during the execution of hand movements. Event-related synchronizations (ERSs), which are increases in power in the brain's beta (12-24 Hz) rhythms, were found to occur when hand movements stop (Pfurtscheller & Lopes da Silva, 1999; Pfurtscheller, Zalaudek, & Neuper, 1998). These ERDs and ERSs were found to be more pronounced in faster hand clenching movements (Yuan, Perdoni, & He, 2010). Other EEG studies have also shown that self-initiated hand movements and tasks involved with moving fingers in particular sequences involve brain activity near the frontal regions (Bortoletto, Cook, & Cunnington, 2011; Gerloff et al., 1998). While these neuroimaging studies have shown generalized brain activity changes related with hand movements, it is desirable to study how the brain controls the finer tuning of hand movements such as those involved in dexterous grasping or in delicate and timely finger tapping tasks.

In this regard, neural decoding approaches have been pursued to examine the nature of the neural representation for the control of fine finger movements. Neural spiking activity and local field potentials (LFPs) recorded with surgically implanted microelectrodes on cortical tissue have been used to decode the time course of arm and finger movements as well as identifying which digit was moved (Bansal, Vargas-Irwin, Truccolo, & Donoghue, 2011; Hamed, Schieber, & Pouget, 2007; Vargas-Irwin et al., 2010; Zhuang, Truccolo, Vargas-Irwin, & Donoghue, 2010). While these studies have

yielded reasonably high decoding accuracies, they have typically focused on recording activity from a small population of neurons in the primary motor cortex. Hand movements have also been decoded with brain rhythms recorded on a larger spatial scale with electrocorticography (ECoG); where researchers have been able to decode the time course of the flexion of individual fingers (Kubánek, Miller, Ojemann, Wolpaw, & Schalk, 2009), and the position of individual fingers while subjects were engaged in a slow and deliberate grasping task (Acharya, Fifer, Benz, Crone, & Thakor, 2010). However, to the best of our knowledge, no decoding studies have been pursued to investigate whether finger trajectories can be inferred from noninvasive signals acquired with scalp EEG. Table 1 summarizes finger decoding studies and their decoding accuracies.

Table 1: Summary of finger movement decoding studies			
Task	*Decoding accuracy (Pearson's correlation coefficient)*	*Signal modality, pre-processing and number of subjects*	*Reference*
3D Reach-to-grasp	Monkey C: r = 0.72 Monkey G: r = 0.74 (medians)	Microelectrode; Neuron firing rates; Monkeys C, G	Vargas-Irwin et al., 2010
3D Reach-to-grasp	δ: r = 0.46 (average) γ: r = 0.62 (average)	Microelectrode; LFP data; Monkeys C, G	Zhuang et al., 2010
3D Reach-to-grasp	Position: r = 0.65 (average) Velocity: r = 0.75 (average)	Microelectrode; 0.3-2 Hz LFP data; Monkeys C, G	Bansal et al., 2011
Slow and deliberate grasping task	r = 0.51 (median)	ECoG; 2 s moving average filter; 4 patients	Acharya et al, 2010
Flexion of individual fingers	Thumb, r = 0.56 Index, r = 0.60 Middle: r = 0.54 Ring: r = 0.50 Little: r = 0.42 (averages)	ECoG; 100 ms average window; frequency bins from 8 to 175 Hz, excluding 35-70 Hz, 5 patients	Kubánek et al., 2009

Table 1. Summary of studies where finger movements were decoded from brain signals. The table indicates the decoding accuracy, which modality was used, and what features were used for decoding the finger movements. Decoding accuracies are measured as the Pearson correlation coefficient between the predicted and observed trajectories. The 'δ' and 'γ' symbols in Zhuang et al.'s (2010) study correspond to decoding accuracies obtained from using delta (.3-4 Hz) and high gamma (200-400 Hz) frequencies to decode grasp motion.

The previously mentioned LFP and ECoG studies have found that slow cortical potentials contributed largely to the decoding of hand movements (Acharya et al., 2010; Bansal et al., 2011; Kubánek et al., 2009; Zhuang et al., 2010). These slow cortical potentials are found to modulate in amplitude with hand kinematics. The slow cortical potentials are often extracted from the recorded brain activity by low pass filtering or using a moving average filter on the recorded signals. In the ECoG studies, these slowly oscillating signals are referred as local motor potentials (LMP), which are typically found to be close to the primary motor cortex (Acharya et al., 2010; Kubánek et al., 2009).

1.2. Knowledge Gaps

To our knowledge, there are very few studies where the kinematics of fine individual finger movements have been decoded from brain signals. While these decoding studies have high accuracies, they are inherently limited by the lack of coverage over the entire brain. Microelectrodes typically record neural activity from a few neurons in the primary motor cortex while ECoG studies are limited to electrode placements that are used to monitor brain health in epileptic patients. As indicated by the previously mentioned fMRI and EEG studies, other areas of the brain are involved in finger movements, which could be used to decode finger trajectories. There is a poor understanding on how the entire brain as a whole can be used to decode finger movements.

It is also of interest to see if noninvasive methods, such as EEG, can be used to decode the fine movement of individual fingers. In the scope of neuroprosthetic devices, implementing microelectrode arrays or ECoG to record brain activity presents surgical

risks to the patient. Using noninvasive methods like EEG can provide a more practical and safer alternative, making the neuroprosthetic device more applicable to clinical populations at risk such as children and the elderly.

1.3. Hypothesis

In this study, we investigated the hypothesis that brain signals recorded noninvasively through scalp electroencephalography (EEG) can be used to decode fine finger trajectories.

The hypothesis is based on the rationale that as slow cortical potentials measured with LFPs and ECoG can be used to decode finger trajectories (Acharya et al., 2010; Bansal et al., 2011; Kubánek et al., 2009; Zhuang et al., 2010), it is likely that the information about finger movement can also be extracted from slow neural activity measured with EEG with minimal distortion. In this regard, the invasive studies previously reviewed indicate that detailed information about finger movement is carried in amplitude modulations of the smoothed ECoG or LFP signals in the delta (0.1-4 Hz) bands originating from a small group of neurons in specific and detailed brain regions. Although EEG recordings represent the activity from large and separated groups of neurons, it can be argued that these amplitude modulations can also be recorded from EEG as low-frequency, delta band signals. EEG signals in the delta band are unlikely to be significantly affected by the conductivity of the brain tissues, and are less susceptible to alterations caused by eye or muscular artifacts. Studying these slow cortical potentials with EEG provides the added benefit of being able to record over the entire scalp, capturing brain activity across the entire cortical area. Thus, a secondary aim of this study

is to examine the neural representation of finger movements at the macro-scale of scalp EEG.

1.4. Objectives

In this ‘proof-of-principle’ study, a linear decoder with memory was designed to translate the derivative of the EEG signal into the angular velocity of the metacarpal-phalangeal (MCP) joint of the index finger. The objectives behind this study were as follows:

1) Evaluate the performance of decoding finger movements with EEG signals recorded from the scalp.

2) Provided that the first objective was fulfilled, to find the neural representations involved in the finger movements.

2. Methods

2.1. Recording and Behavioral Task

Five healthy right-handed subjects participated in this study (age 25 ± 2 years, 4 male and 1 female) after giving informed consent as approved by the University of Maryland Institutional Review Board. Since an objective of this study was to compare the decoding accuracy and representation of finger movements at the macro-scale of EEG with respect to ECoG, the experimental protocol followed that as described in Kubánek et al.'s study (2009). Specifically, subjects were instructed to tap their right index finger three times in succession while seated behind a table with their forearms comfortably resting flat on the table. Each trial (consisting of a series of three taps) was self-initiated. EEG and hand kinematics were recorded simultaneously while subjects performed the finger tapping task. EEG signals were recorded over the entire scalp using a 64 channel HydroCel Geodesic Sensor Net (Electrical Geodesics, Inc., Eugene, Oregon). The recorded EEG signals were amplified and digitized at 500 Hz with Net Amps 300 (Electrical Geodesics, Inc., Eugene, Oregon). Trajectories of 18 joint angles were recorded with a wireless data glove (CyberGlove, Immersion Inc., San Jose, California) at a resolution of 0.93° at a non-uniform sampling rate of 35-70 Hz. The glove was calibrated once for each subject by manually adjusting the gain and offset of each glove sensor's raw value and by visually verifying that the joint angles between the virtual hand and the actual hand matched. Subjects were recorded for approximately 10 minutes each, which recorded ~100-200 trials. The first 100 trials that were completed correctly (which did not include trials where subjects accidently tapped more or less than three times) were

used in the following decoding steps. The experimental set up and examples of the glove recordings while the subject performed the task are shown in figure 1.

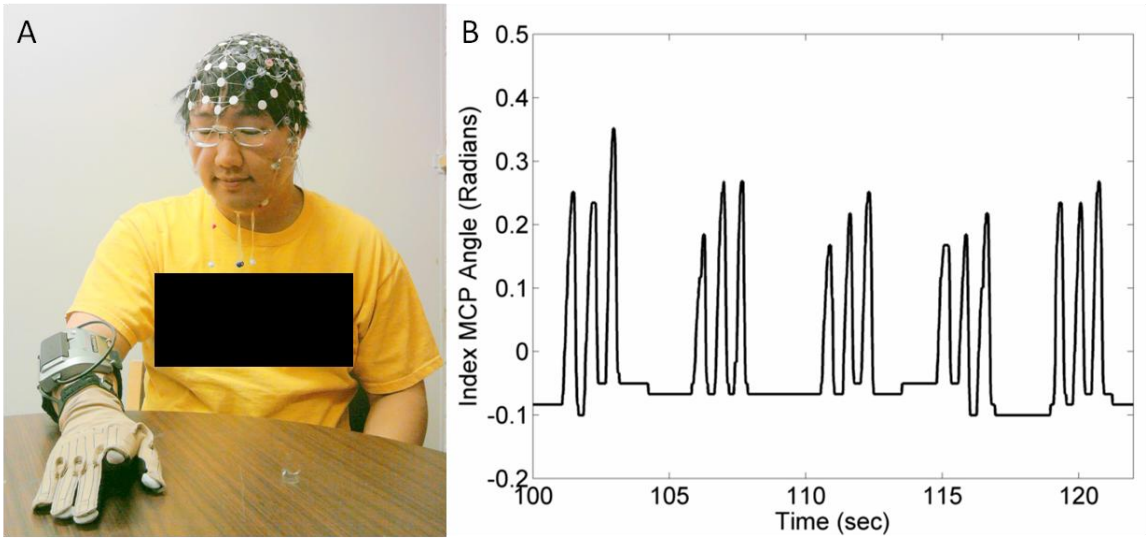

Figure 1. Experimental set up for the behavioral task and examples of glove recordings. A) Photograph of a subject wearing the EEG cap (Electrical Geodesics, Inc., Eugene, Oregon) and the data glove apparatus (CyberGlove, Immersion Inc., San Jose, California) while performing the finger tapping task. B) Examples of the angular trajectories recorded from the glove sensor located at the index metacarpal-phalangeal (MCP) joint.

2.2. Data Synchronization

To synchronize the EEG recordings with the kinematics recordings, a video of the session was recorded at 30 frames per second. The video was assumed to be synchronized with the EEG internally by the recording software (NetStation 4.3, Electrical Geodesics Inc.). The video, along with the glove software, simultaneously recorded the on and off status of a red LED, which was mounted on the glove. Manually

turning the LED on and off three times consecutively served as event markers to synchronize the glove data and the video.

The raw synchronized EEG and kinematics recordings were resampled at 100 Hz in the following manner. A Chebychev II antialiasing filter at 40 Hz was applied to the raw EEG signals followed by a down-sampling to 100 Hz. The raw kinematics signals were interpolated with a piecewise cubic hermite interpolating polynomial and up-sampled to 100 Hz.

2.3. Kinematics Analysis

To observe the variation of the finger tapping motion across subjects, different measures of the finger tapping motion were calculated for each trial including: trial length, tapping speed, resting position, extension angle, and range of motion. The average, standard deviation, and coefficient of variance of these measures were calculated across all trials for each subject. The statistics of these measures are shown in Table 2.

Temporal properties of the finger tapping motion were measured by calculating the trial lengths and tapping speed of each trial. The trial length was approximated by finding when the tapping motion started, called the movement onset time, and finding when the tapping motion ended, called the movement offset time. Movement onsets were determined to be time points at which the joint angle speed exceeded 5% of the maximum velocity for the first time during a trial. Similarly, movement offsets were determined to be time points at which the joint angle speed was within 5% of the maximum speed for the last time near the end of the trial. Subtracting the movement

onset time from the movement offset time of each trial yielded the trial length. For each trial, dividing the number of taps (three) by the trial length yielded the approximate tapping speed.

The angular properties of finger tapping motion were measured by calculating the resting position, the extension angle, and the range of motion of each trial. The resting position of each trial was approximated by taking the average of the finger positions in a one second segment located before the beginning of each trial and after the end of each trial. To find the extension angle of each trial, the three local maxima in the low pass filtered finger trajectories were located to extract the time points of full finger extensions (Smoothing the trajectories with a low pass filter facilitated the process in finding the locations of the local maxima). The amplitudes of the unfiltered finger trajectories at these time points were extracted as the extension angle (The local maxima in the filtered trajectories were not used because they were often lower in magnitude than the local maxima in unfiltered trajectories). The three local maxima were averaged, giving the approximate extension angle for that trial. The range of motion of each trial was calculated by subtracting the resting position from the extension angle.

The power spectral density (PSD) of the kinematics was also calculated. First, the index finger trajectory data across the recording session containing the first 100 trials was detrended from the mean. The PSD of the data was calculated by using the Thomson Multitaper method PSD function in MATLAB (MathWorks, Inc., Natick, Massachusetts). A time bandwidth product of 4 and the Fourier transform window length of 512 were used.

2.4. Preprocessing

Before designing and calibrating the decoder using the index finger's trajectories and the EEG data, both data sets were preprocessed. A flow chart of the preprocessing steps is shown in Figure 2.

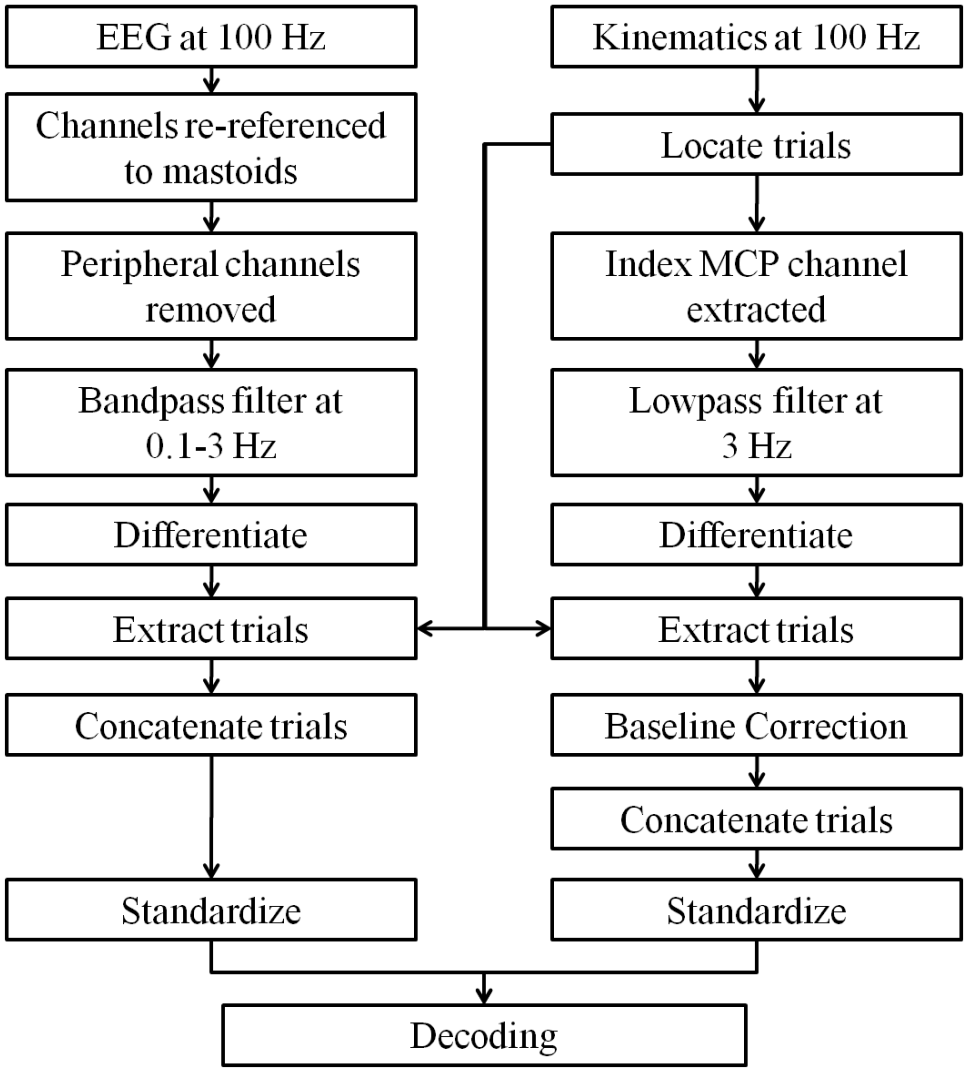

Figure 2. Flow chart indicating the preprocessing steps used in this study.

First, EEG recordings were re-referenced from a Cz reference to the mastoids. EEG signals from eighteen peripheral channels along frontal and temporal sites were

rejected. The rejected channels are shown as red labels in figure 3B. These channels were removed because they were most likely to be strongly influenced by eye artifacts or muscular artifacts due to head movements. The EEG recordings were then high pass filtered at 0.1 Hz with a zero-phase 4th order Butterworth filter. Only the data from the metacarpal-phalangeal (MCP) joint of the index finger was used in the study, so the kinematics data from the other channels were removed. The sensor associated with the metacarpal-phalangeal joint of the index finger is indicated with a red circle in figure 3C.

Next, both EEG and kinematics recordings were low-pass filtered at 3 Hz (i.e., within the delta band) with a zero-phase 1st order Butterworth filter. The EEG signals were low pass filtered to remove noise and other high frequency brain activity unrelated to finger movements. The kinematics signals were low pass filtered to smooth the step-like structure introduced by the glove's resolution limits. The low pass cut off frequency for the EEG and kinematics was determined by estimating the fastest speed of the tapping motion across all subjects, which was found to be approximately 2.5 Hz. This was further confirmed by visually inspecting the power spectral densities of the MCP joint kinematics and by inspecting the index finger trajectories after the filter was applied. A cut off frequency of 3 Hz was found to reasonably preserve the tapping trajectories. After the data was filtered, the numerical derivative of the EEG and the kinematics recordings were calculated.

After filtering, the EEG and kinematics were transformed into their derivatives. Using the derivative of the EEG and kinematics in preliminary decoding attempts was found to increase decoding accuracy.

The continuous EEG and kinematics were then extracted into segments consisting of the movement period from 0.1 seconds before the beginning of each trial to 0.1 seconds after the end of each trial (The beginning and end of each trial correspond to movement onsets and movement offsets as described in section 2.3). Across subjects, the average length of the trial was found to be 1.84 seconds (giving an average segment length of 2.04 seconds across subjects). Any data outside of the movement periods were not used for further analysis. The segmentation provided a balanced representation of movement and rest for the decoder. The segmented kinematics data was baseline corrected by the mean of the segment -0.1 to 0 seconds with respect to the beginning of the trial. This was done to reduce the effects of the gradually increasing magnitudes found in the kinematics data throughout the recording session. After segmenting, the data was concatenated and standardized with respect to the means of each channel. Examples of the data are shown below in figure 3.

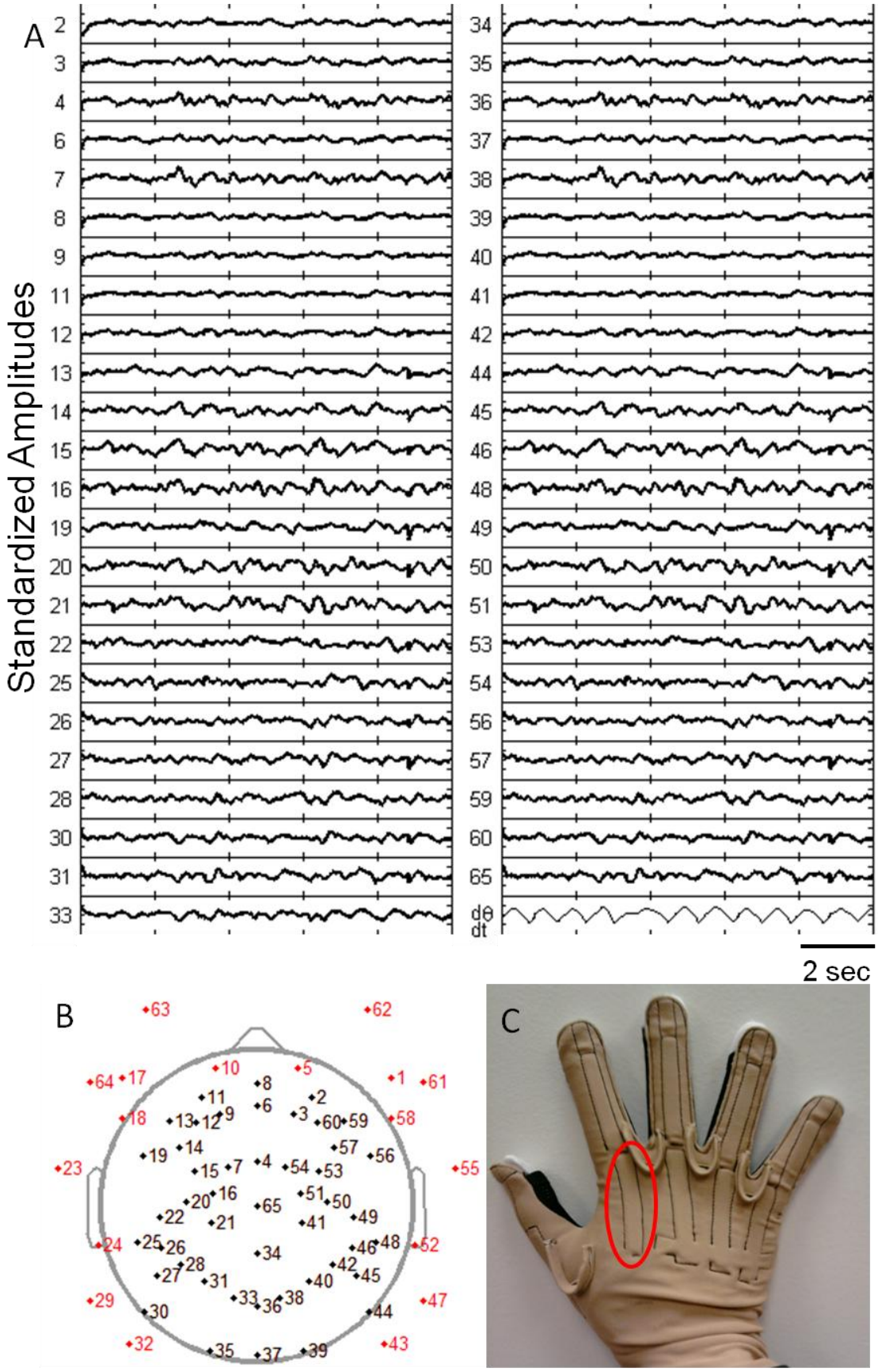
A
Standardized Amplitudes
2 sec
B
C

Figure 3. Examples of the preprocessed EEG and kinematics signals used in the study. A) The EEG signals are plotted as a thick black line while the index finger trajectory is plotted as a thin black line. Signals are preprocessed as mentioned in the steps above. B) Locations of the EEG channels are plotted as shown. The black and red labeled channels are channels which were respectively included and removed from the study. C) Photograph of the data glove apparatus (CyberGlove, Immersion Inc., San Jose, California) used in the study. The circled area indicates the sensor used to record the angles of the index MCP joint.

2.5. Decoding Kinematics from EEG

2.5.1. Linear Decoder

A linear decoder was used to decode the index MCP joint angular velocity from the derivative of the EEG signals. The overall paradigm involved using the magnitudes from EEG signals from certain channels at different temporal points in the past to calculate the present joint angular velocity. EEG sensors to be chosen for decoding were selected through a genetic algorithm that found an optimal set of channels which maximized decoding accuracies (see section 2.5.3 for further details). The index MCP joint angular velocities were modeled as a linear combination of data from the selected sensors:

$$\theta'(t) = \sum_{i=1}^{N} \sum_{k=0}^{L} b_{ik} S_i^{'}(t-k)$$

where $\Theta'(t)$ is the angular velocity of the index MCP joint at time t, i corresponds to a certain ith sensor where N is the total number of sensors (N=47), k is the temporal lag in

milliseconds which creates an offset between the EEG and kinematics signal where L is the total number of lags (L=7), b_{ik} is the weight which is the coefficient that is multiplied by the magnitude of the ith sensor at a certain time lag k, $S_i'(t-k)$ is the magnitude of the EEG sensor's derivative from ith sensor at time t-k, and t is the time in milliseconds. The data was decoded with multiple lags where k = 0, 50, 100, 150, 200, 250, and 300 ms in the past.

2.5.2. Model Training and Validation

The performance of the model was evaluated using the 10-fold cross validation scheme. The flow chart for the scheme is shown in figure 4.

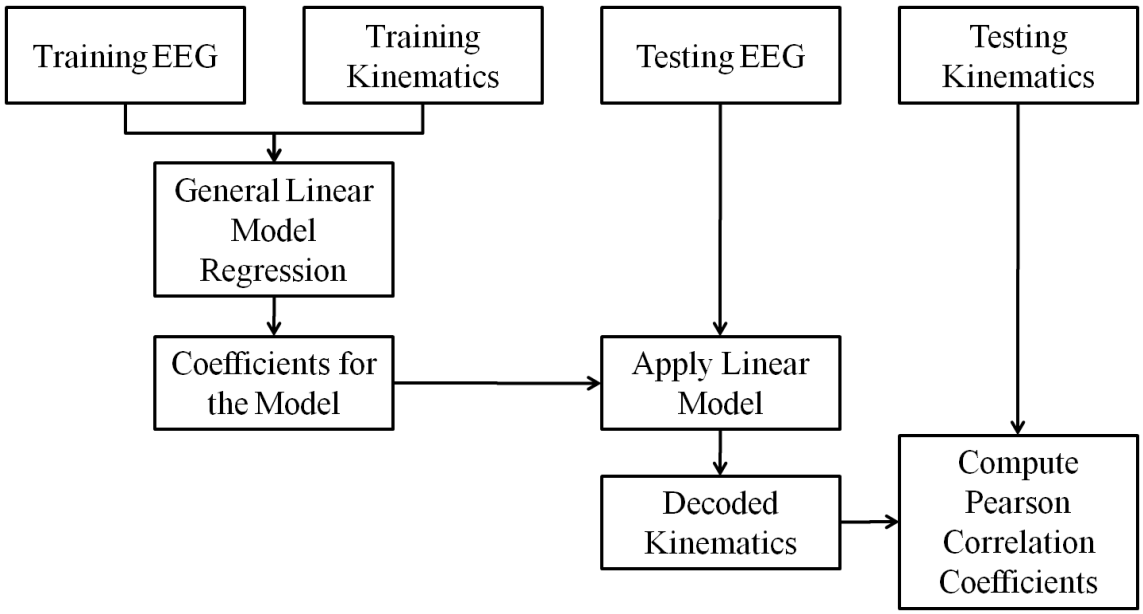

Figure 4. Flow chart of the cross validation scheme. To maximize generalization, the collected data was divided in training and testing data for purposes of decoder calibration and decoder cross-validation (see text for details).

100 trials of each subject were used to train and test the linear decoder. For each fold, the data was split into 10 groups, 9 of which were used to train the linear decoder while the remaining group was used to test the decoder. Each group consisted of 10 trials. The weights b_{ik} of each channel from each lag were calculated as the coefficients which fit a linear model between the EEG signals and the kinematics signals from the training trials. The weights b_{ik} were calculated using GLM (Generalized Linear Model) functions in MATLAB (MathWorks, Inc., Natick, Massachusetts). Using the calculated weights from the training data, the linear decoder was used with the EEG data from the remaining training group to predict the observed joint velocities in the same training group. The predicted trajectories were then standardized and low pass filtered according to the preprocessing steps. The Pearson correlation coefficient, which was used as the performance metric, was calculated between the predicted trajectories and the observed trajectories. This is repeated for each fold, each of which consisted of different training and testing groups of trials.

2.5.3. Channel Selection

Previous decoding studies have found that an ideal number of electrodes or neurons were needed to fully decode the trajectories of hand movements (Acharya et al., 2010; Bradberry et al., 2010; Hamed et al., 2007). In a previous study from our lab, we found that decoding accuracies begin to decrease after an optimal set of channels were used, possibly due to overfitting of data in the training sets (Bradberry et al., 2010). In this study, we decided to explore the use of the genetic algorithm to find an optimal set of channels to be used in decoding. Genetic algorithms are widely used for numerical

optimization purposes (Haupt, R & Haupt, S., 2004). In the context of this study, the genetic algorithm found the optimal set of channels, which yielded the highest decoding accuracy. To implement the genetic algorithm, an individual within a population was designated to be a set of EEG channels to be used in the decoding. Individuals whose channel sets yielded the highest decoding accuracy were preserved throughout the next generation. The genetic algorithm was implemented with the genetic algorithm functions in MATLAB (MathWorks, Inc., Natick, Massachusetts). An example of the how the population evolves throughout the generations is shown below in figure 5. Initially, individuals began with a random combination of channels to use. As the genetic algorithm progressed through the generations, the decoding accuracies of the populations increased, and few channels were selected by most of the individuals. The fitness value of an individual, which determined if its channel set was preserved through the next generation, was calculated as the median of the correlation coefficients across the 10 folds used in the cross validation scheme (as discussed in section 2.5.2).

It should also be noted that the genetic algorithm also selected which temporal lags should be used for each channel. Thus, each individual selected 329 different channels and lags (arising from the use of 47 channels and 7 lags for each channel) to potentially be used as part of the decoding. Technical parameters used for the genetic algorithm are shown in table 3 in the appendix.

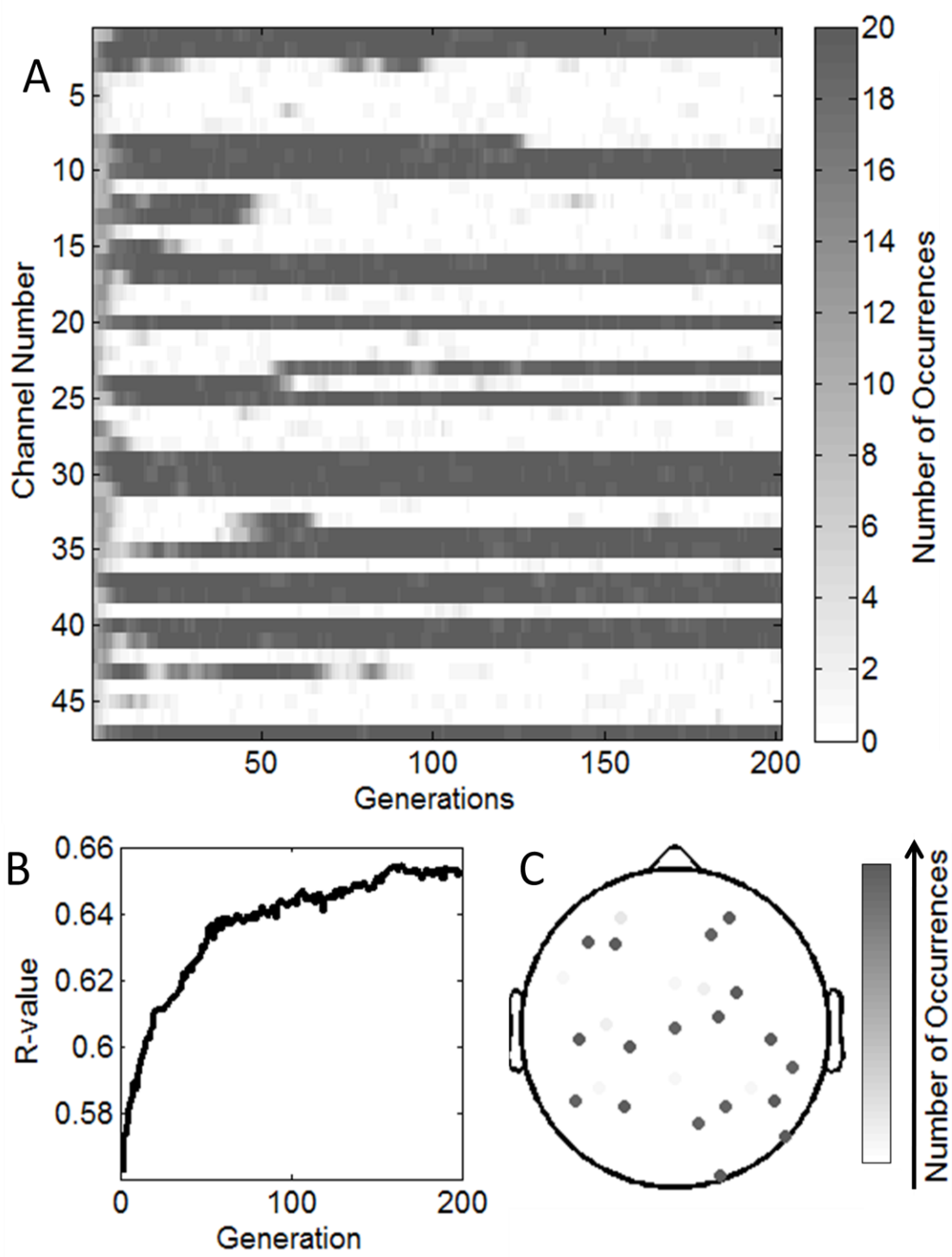

Figure 5. Example of the progression of the genetic algorithm, showing the evolution of channels selected for one temporal lag across generations. A) Number of times each channel was selected across individuals from each generation. Darker colors indicate that

more individuals within a generation selected that particular channel. B) The median fitness value across all individuals increases through the progression of generations. C) Scalp map depicting how many times a channel is selected by all individuals in the last generation. As shown in A), darker channels indicate that more individuals in the last generation selected a channel.

2.6. EEG correlations with finger trajectories

To gain a better understanding of the weights found in the decoding, an analysis was done to determine which channels had slow cortical potentials that modulated in amplitude with the finger trajectories. The Pearson correlation coefficient was calculated between preprocessed EEG signals from each channel and the finger tapping trajectories. This was repeated with the same temporal lags used in the decoding methods stated above.

3. Results

3.1. Kinematics Statistics

Table 2 shows the statistics of the tapping task performed by the subjects. We note the wide variability across subjects on the full range of motion (ROM) and in the tapping speeds. Figure 6 shows the power spectral densities of the raw finger trajectory data. The calculated tapping speeds as well as the power spectral density suggest most of the variation in the raw finger trajectories was less than 3 Hz, justifying the low pass filter cut off frequency for both the EEG and the finger kinematics in the preprocessing steps.

Subject	*Extension (Degrees)*	*Rest (Degrees)*	*ROM (Degrees)*	*Trial Length (Sec)*	*Tapping Speed (Taps/Sec)*
1	17.31 (4.21) 0.24	-22.33 (5.54) 0.25	39.64 (4.46) 0.11	1.43 (0.12) 0.08	2.11 (0.17) 0.08
2	9.45 (6.03) 0.64	-25.20 (6.35) 0.25	34.65 (4.16) 0.12	1.27 (0.10) 0.08	2.37 (0.17) 0.07
3	14.56 (2.74) 0.19	-6.96 (2.77) 0.40	21.52 (3.26) 0.15	2.12 (0.15) 0.07	1.42 (0.10) 0.07
4	24.63 (3.69) 0.15	-22.39 (1.00) 0.04	47.01 (3.53) 0.08	1.93 (0.30) 0.16	1.59 (0.23) 0.14
5	27.82 (2.71) 0.10	-17.08 (2.28) 0.13	44.90 (2.80) 0.06	2.44 (0.28) 0.11	1.25 (0.13) 0.10
All	18.76 (7.81) 0.42	-18.79 (7.67) 0.41	37.55 (9.82) 0.26	1.84 (0.48) 0.26	1.75 (0.46) 0.26

Table 2. Statistics of the finger tapping task. For each subject, the average values are shown at the top, the standard deviation is shown in the middle in parenthesis, and the

coefficients of variation is shown in the bottom and underlined. The data glove apparatus measures the index MCP joint angle such that when the index finger is parallel with the palm, the joint is measured as 0 degrees. When the finger extends away from the palm, it is measured in positive degrees. When the finger flexes towards the palm, it is measured in negative degrees.

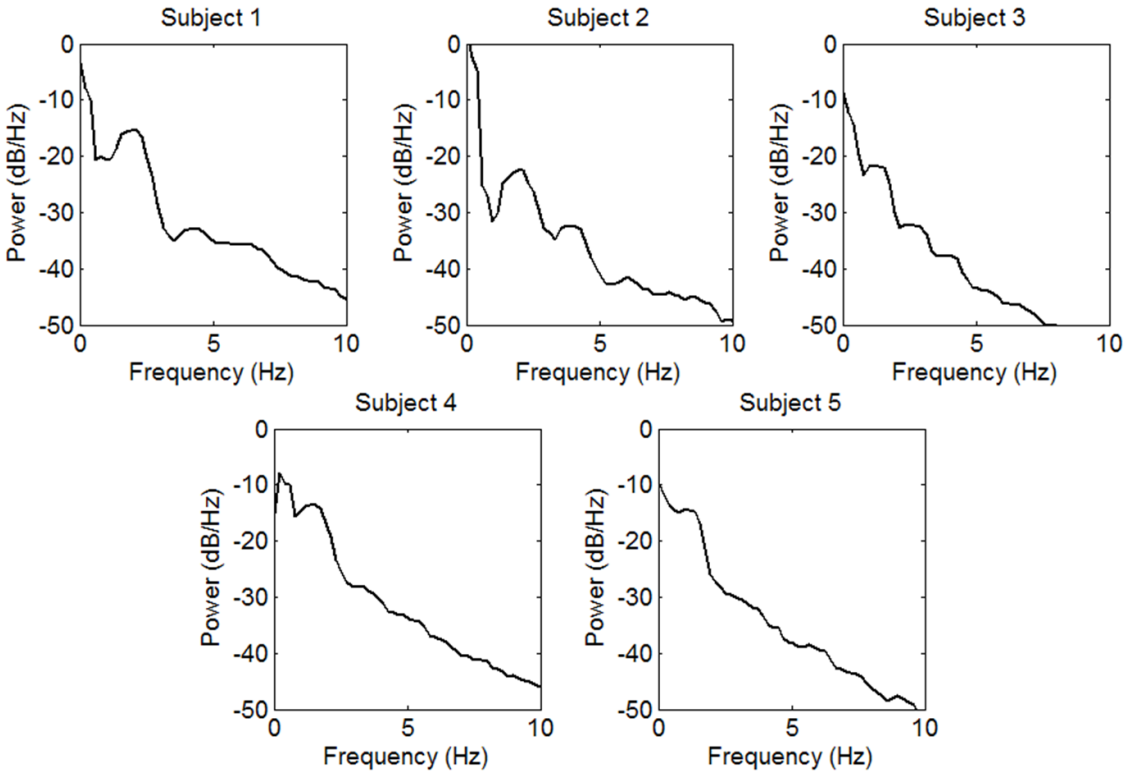

Figure 6. Power Spectral Densities of the index finger MCP joint trajectories throughout the recording session. The plots are smoothed over 5 samples to help visualization.

3.2. Decoding Performance

The EEG decoder was able to infer movement of the MCP index finger velocities from the derivative of the EEG signals. Figure 7 shows examples of the observed and predicted joint velocity kinematics. The predicted trajectories appear to follow the

general path of the observed trajectories. As shown in figure 8, the decoding performance varied across subjects with a median of r = 0.403 and a maximum of r = 0.704. All correlation coefficients between the predicted and observed trajectories were found to be significant ($p<0.001$).

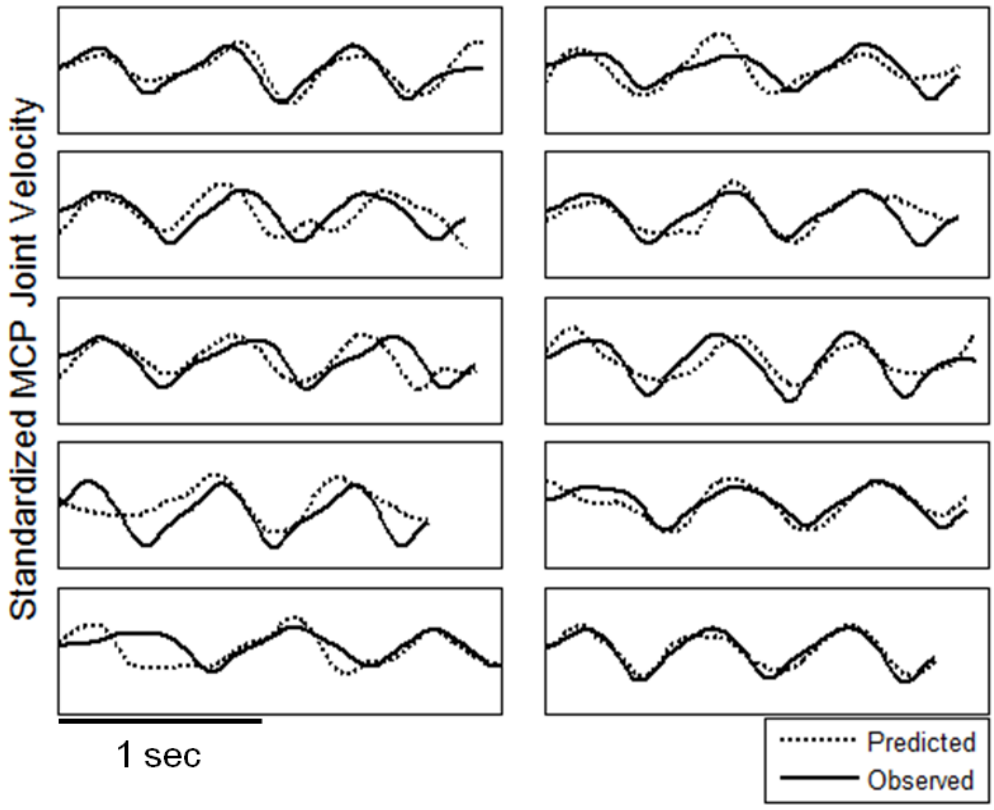

Figure 7. Examples of observed and predicted trajectories taken from the fold with the highest decoding performance (r=.704, Subject 3). The decoded trajectory is shown as a dotted line while the observed trajectory is plotted as a solid line. The plotted trajectories were standardized and low pass filtered.

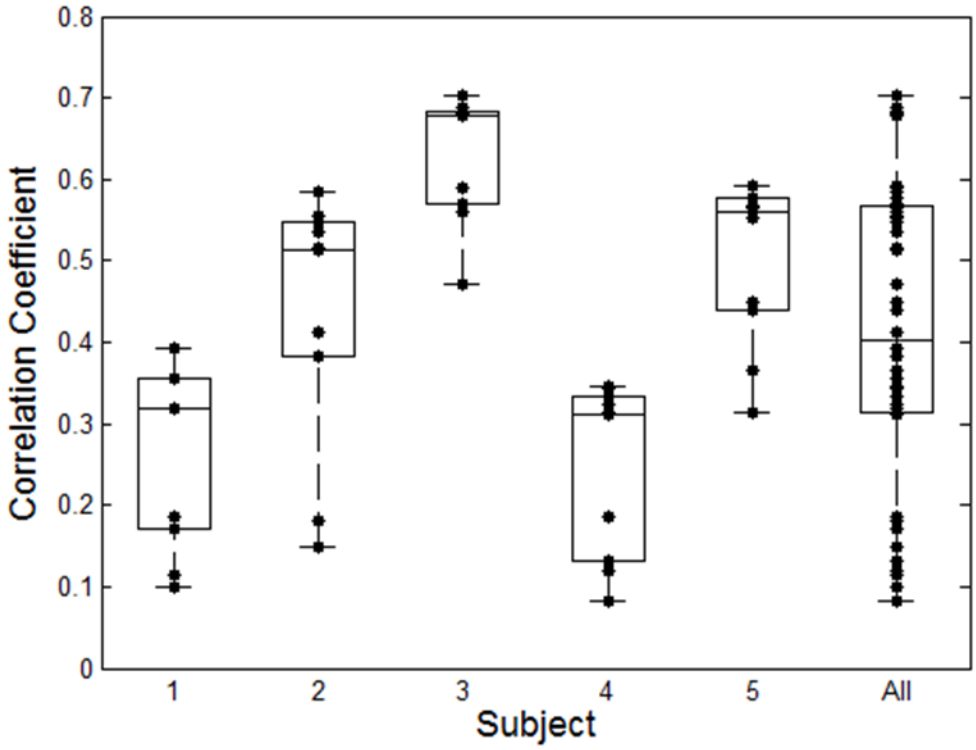

Figure 8. Boxplots of Pearson correlation coefficients of the decoder's predicted trajectories against the observed trajectories across the 10 folds for all subjects. Individual r-values from the 10 folds are plotted as dots overlaid over the boxplots. The boxplot on the right describes the distribution of r-values from all subjects.

3.3. Channel Weights

The decoding scheme involved creating an optimal set of channels across all lags to predict the joint velocity from the EEG data. Different weights were placed on different channels, where the signals from certain channels contributed more to the decoded trajectories than other channels. Shown in figure 9 are the weights of the channels across all subjects. Within each subject, the channel weights were normalized to show which channels contributed the most to decoding the finger trajectories. To observe

the overlap of the channels weights across lags and subjects, the normalized weights were averaged. The scalp maps on the right column and bottom row, respectively, show the normalized weights averaged across the subjects and across the lags. The scalp map on the bottom right shows the gross average of the normalized channel weights across both lags and subjects. Channels which were removed by the genetic algorithm were plotted as white points. To calculate the contribution of the EEG signals from each lag to the decoding, the weights within each lag were summed for each subject, and the sum of the weights of each lag were divided by the total sum. The lag contributions are plotted in figure 10.

We found that the distributions of the channel weights varied considerably across subjects. For subjects 1 and 4, the higher weights appeared to be concentrated near the ipsilateral side of the frontal lobe and weighed most heavily at lags -50 and 0 ms. For subject 2, the higher weights were found on the contralateral side of the scalp near the frontal lobe: near the central part of the brain at a lag of -50 ms, and around the frontal part of the brain at a lag of -200 ms. In subject 3, the heaviest weights were scattered in the medial part of the brain, with a concentrated cluster on the contralateral side of the frontal lobe. The weights were concentrated heavily at 0 ms. In subject 5, the heaviest weights were found at in the middle of the frontal lobe at a lag of -300 ms.

For subjects 1 and 3, the 0 ms lag contributed most to decoding. For subjects 2 and 4, the 50 ms lag contributed the most to decoding. For subject 5, the -300 ms lag contributed the most to decoding.

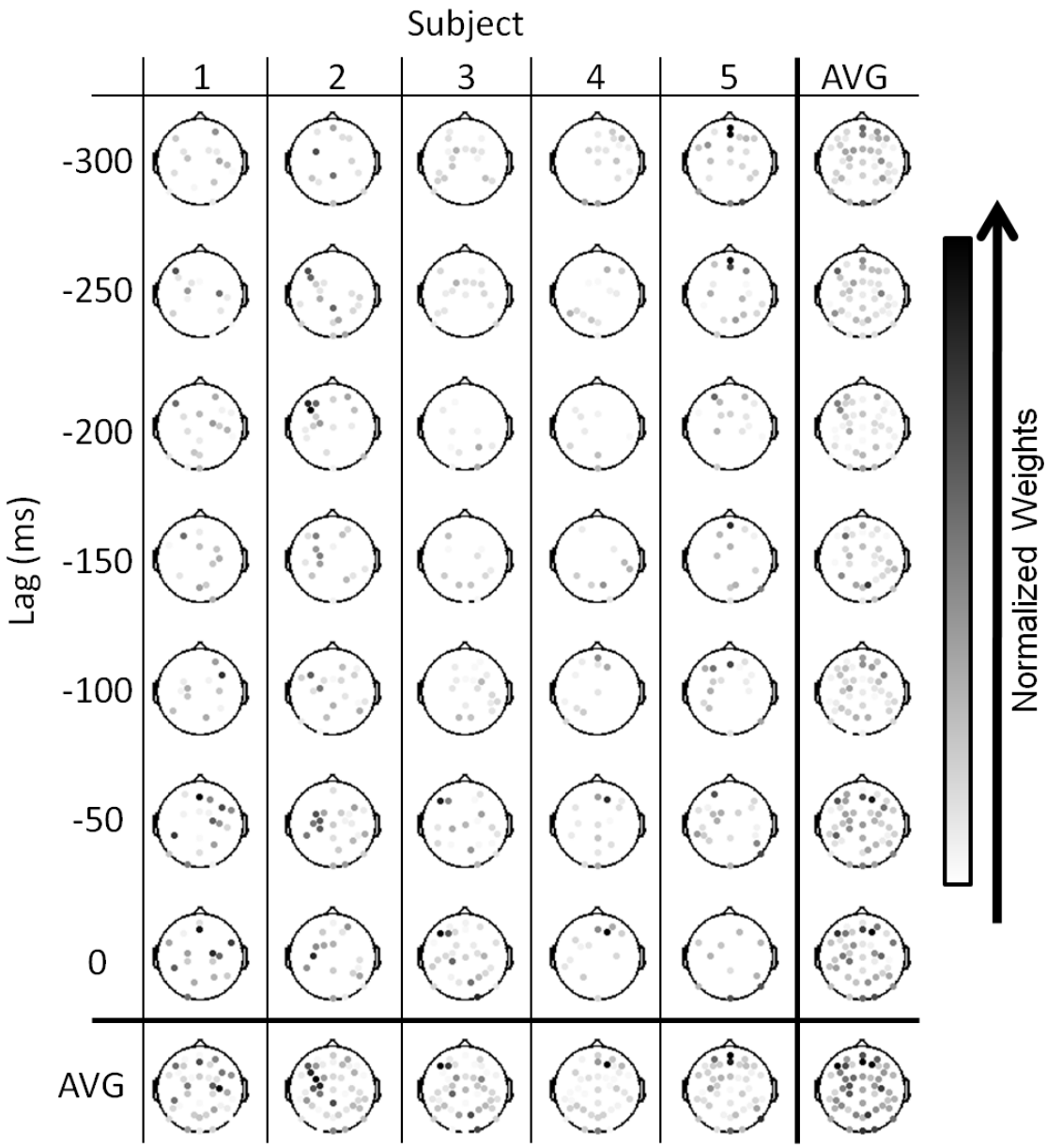

Figure 9. Raster plot of scalp maps plotting the normalized weights of all the channels. The right column and bottom row show the averages of the normalized channel weights respectively across subjects and lags. The bottom right scalp map shows gross average of all the normalized channel weights. All plotted values are normalized with respect to the maximum weight across all scalp maps enclosed within the lines. Darker points indicate a higher weight on the channel.

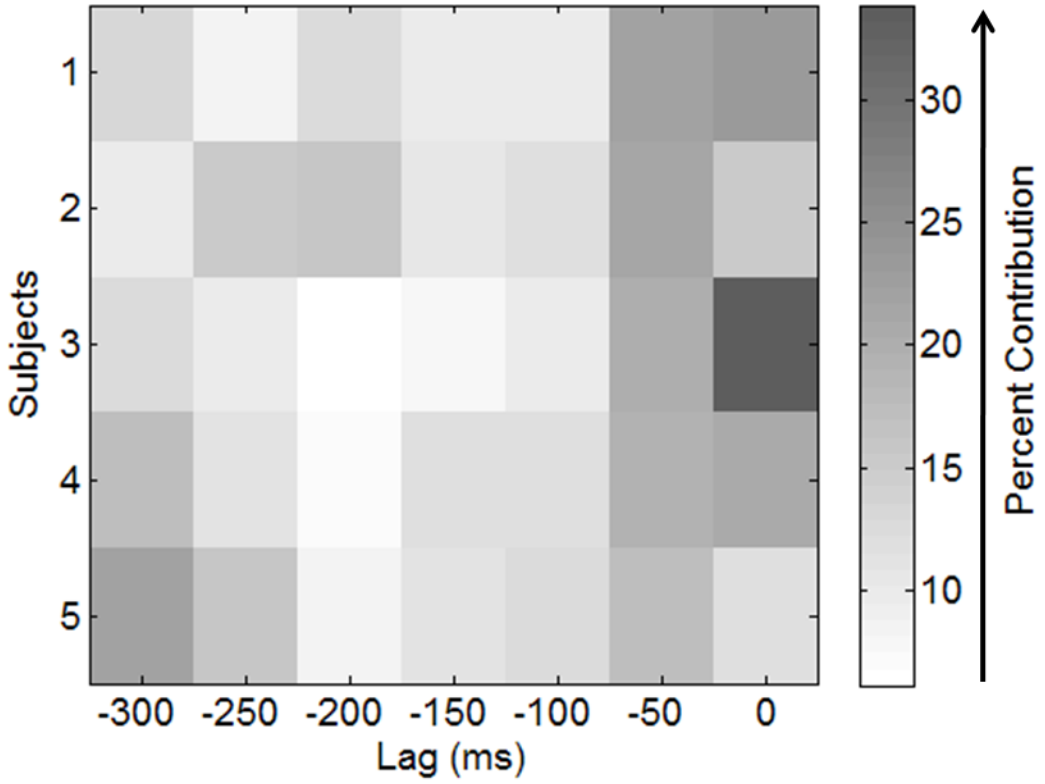

Figure 10. Weight contributions of each lag across subjects. Darker colors indicate a larger sum of channel weights for that lag, implying a larger contribution of that lag to decoding.

3.4. Channel Correlations with finger trajectories

Figure 11 shows the raster plot of Pearson correlation coefficients between the preprocessed EEG signals from each channel with different lags and the finger kinematics. The scheme where values were averaged across lags and subjects, as well as the normalizations, were the same as that used in plotting the decoder weights in figure 9. For subject 1, the most correlated channels were found on both sides of the frontal site at lags -150 and -200 ms. For subject 2, the most correlated channels were located on the

contralateral side of the motor cortex centered at lags -200 ms and 0 ms. For subject 3, the most correlated channels appeared at both sides of the motor cortex across at lag 0 ms and at the contralateral motor area at lag -300 ms. For subject 4, the most correlated channels appeared at both sides of the motor cortex, being most heavily correlated at lags -100 and -50 ms. For subject 5, the most correlated channels were found on the contralateral side of the motor cortex, at lags -150 ms and -100 ms.

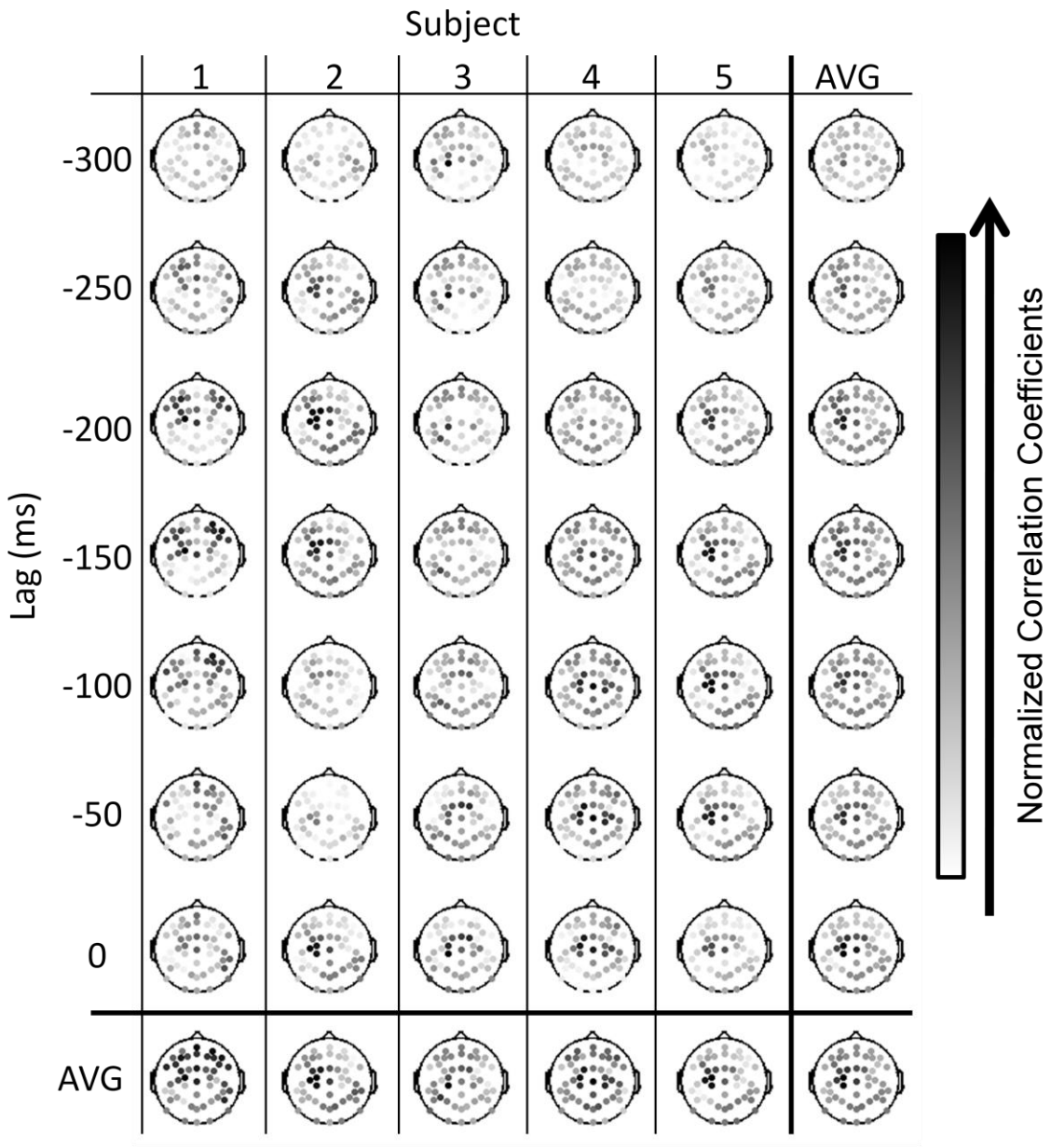

Figure 11. Raster plot of scalp maps plotting the normalized Pearson correlation coefficient between each channel from each lag and the index finger trajectories. The right column and bottom row show the averages of the normalized correlation coefficients respectively across subjects and lags. The bottom right scalp map shows gross average of all the normalized correlation coefficients. All plotted values are

normalized with respect to the maximum weight across all scalp maps enclosed within the lines. Darker points indicate a higher correlation coefficient.

4. Discussion

The main finding of this study is that the finger joint velocities of the MCP joint during finger tapping can be inferred from a plurality of noninvasive scalp EEG signals with the same degree of accuracy as invasive approaches that record brain activity under the dura or intra-cortically using microelectrode arrays (Acharya et al., 2010; Bansal et al., 2011; Kubánek et al., 2009; Vargas-Irwin et al., 2010; Zhuang et al., 2010).

4.1. Decoding Performance

The decoding accuracies found in this study are comparable to that of other studies which decoded finger movements through ECoG and microelectrode recordings (Acharya et al., 2010; Bansal et al., 2011; Kubánek et al., 2009; Vargas-Irwin et al., 2010; Zhuang et al., 2010). Factors which may have contributed to decoding performance variability included movement variability, changes in internal states (e.g., fatigue, lack of attention or motivation, boredom), and the presence of eye or head movement artifacts. Such factors may have interfered with predicting the trajectories accurately and may also have compromised the ability of the genetic algorithm to select the subset of optimal channels. The results in the study present a realistic situation where these factors may influence the EEG signals.

We also found the subjects with the slowest tapping speeds had the highest decoding accuracies. This has also been observed by Acharya et al. (2010) where the LMPs recorded from ECoG correlated more with slower grasping motions. It is not clear why this trend occurs and presents a limitation to the theory that certain brain activity oscillations modulate in amplitude with finger movements. It suggests that these

matching modulations between brain activity and movements are only prevalent for slower movements.

Based on the coefficients of variations in the kinematic measures, there did not appear to be a trend between the consistency with which each subject performed the finger tapping movement and the decoding accuracies.

4.2. Use of the Genetic Algorithm

This study used a genetic algorithm to test a variety of sensor combinations across different temporal lags to predict finger kinematics from EEG. This was done to take advantage of possible synergies between different EEG electrodes and temporal lags, which may increase decoding performance. Previous decoding studies utilized a neuron or sensor dropping analysis, showing that trajectories can be decoded with a few neurons or sensors (Acharya et al., 2010; Bradberry et al., 2010; Hamed et al., 2007). In our previous work with decoding reaching hand movements from EEG, we found that an ideal number of sensors were needed to have optimal decoding performance; where more sensors were needed to provide sufficient amount of information to the decoder, while having too many sensors compromised decoding performance due to overfitting of the input data (Bradberry et al., 2010). While the genetic algorithm in this study provided a set of channels that yielded the highest decoding performance, it is uncertain if all the channels in the optimal set were necessary to maintain the performance. As shown in figure 9, only a few channels were weighed heavily, while many others were weighed by a small amount.

4.3. Channel weight distributions

We found that the decoders had a general tendency to weigh channels the heaviest near the -50 to 0 ms lags. This is consistent with Kubánek et al.'s (2009) study, where the optimal temporal lag to decode from was at -50 ms. However, previous ECoG studies which decoded finger movements tended to weigh their predictions heavily on electrodes placed on the primary motor cortex on the contralateral side of the hand movements. In this study, only subject 2 had this kind of spatial distribution. The other subjects tended to have frontal lobe channels weighted heavily. This difference in spatial distribution may be due to the fact that the behavioral task involved in this study was self-initiated and involved tapping in a consistent sequence (a burst of three taps). Previous EEG studies have found that the frontal lobes tend to become more activated when subjects were required to self initiate finger movements, or when they were instructed to perform specific finger movement sequences (Bortoletto et al., 2011; Gerloff et al., 1998). We also note that the measured brain activity in this study may have been affected by feedback associated with the task such as the tactile feedback of the finger hitting the table or the auditory tapping noise.

We note however, that in calculating the correlation coefficients between the EEG channels with the finger trajectories, it was found that the most correlated channels tended to cover the contralateral side of the motor cortex. The distribution of the decoder weights did not appear to match such a distribution. One potential explanation is that as nearby electrodes in contralateral motor cortex are likely to be highly correlated to each other due to EEG volume conduction (due to signal propagation in a conductive

medium), the genetic algorithm was able to remove those channels with highly mutual information, resulting in a sparse network for decoding.

Overall, the weight distributions vary widely among subjects. It can be argued that the neural representations between individuals should vary because of physiological differences between individuals. Each subject may have also used different cognitive strategies to perform the task. In any case, the variations in the weight distributions found in this study make it difficult to ascertain which brain areas are consistently involved with finger movements.

4.4. Applications to brain machine interfaces

A brain-machine interface (BMI) is a communication pathway between the brain and an external device, which can restore motor function in an individual (Hochberg et al., 2006; Leuthardt et al., 2004). A BMI system requires a neural interface that can translate brain activity into movement intentions. The results of this study can readily be implemented in a BMI. Designing a BMI system that decodes movement trajectories from scalp EEG presents its advantages. As others have previously argued, BMIs that can decode trajectories of limb movements are a favorable alternative to BMI that rely on operant conditioning or biofeedback because they provide a more intuitive approach for patients training with the BMI (Acharya et al., 2010; Bradberry et al., 2010). The use of noninvasive scalp EEG signals also removes the surgical risks found in other brain activity recording techniques like ECoG or microelectrode implantations. While the results of this study show feasibility for an EEG-based BMI that can control a hand-based prosthesis, further decoding studies should involve tasks that involve the whole hand in

naturalistic conditions. Thus, behavioral tasks that study more natural and dexterous hand movements need to be investigated as well.

4.5. Future Studies

4.5.1. Closed-loop BMI with a hand prosthesis

To assess whether the results of this study can be used for BMI, the performance of a fully realized system where the subject attempts to control a hand-like prosthesis device in real time should be studied. A generic flow chart showing an example of such a system is shown in figure 12.

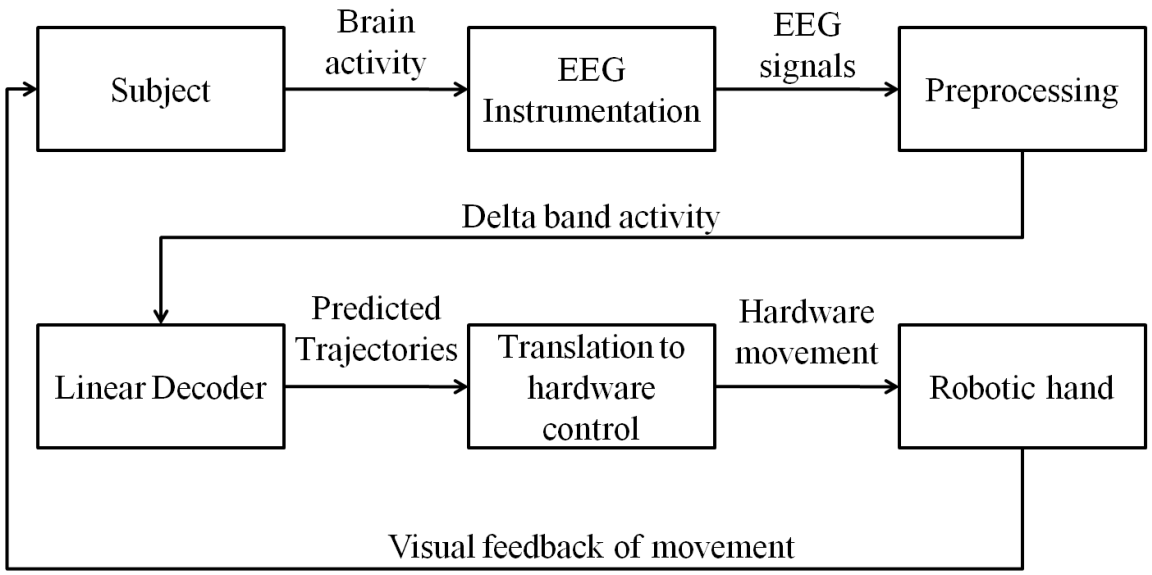

Figure 12. Flow chart of the closed-loop BMI system where the subject controls a robotic hand.

In this closed-loop system, the subject would attempt to move the robotic hand solely through brain activity. As the subject performs the task, EEG signals would be recorded from the subject. The EEG signals can be preprocessed in a similar manner as

was done in this study. These preprocessed signals, which would be re-referenced, bandpass filtered, and transformed into the derivative, would contain the relevant delta wave activity to serve as the appropriate input for the linear decoder. The linear decoder would then multiply the preprocessed EEG signals with the weights found in the training steps from this study. The weights to be used in this study could come from the cross validation fold that performed the best as they may reflect the most relevant neural representation involved with finger movements. (While the weights in this study reflected standardized EEG signals, they can readily be converted to reflect raw signals from the mean and standard deviations of the raw signals). The predicted trajectories would then be transformed into a signal which drives the motors or actuators that move the robotic hand. The subject can then observe the movements of the robotic hand, providing visual feedback which may be necessary for finger movements.

Unlike this study, the performance of the closed-loop BMI system cannot be evaluated by comparing predicted trajectories with observed trajectories since the intended trajectories would not exist. Instead, the performance could be evaluated by observing how accurately the subject can perform the behavioral task. Performing the task correctly could involve goals such as tapping exactly three times, extending the finger past a certain angle, or starting and stopping the tapping motion at correct temporal points. With respect to these goals, performance accuracy can be measured as the number of times the robotic finger taps, the angle of the robotic finger extensions during the tapping motion, and the time duration of how long the robotic finger performs the tapping motion. Comparing these measures with the values set by the goal can quantify how well

the subject can control the prosthetic hand. Lastly, an overall survey on the subject's comfort with the prosthetic limb can be documented.

4.5.2. Studies for a clearer neural representation

The findings of the neural representation in this study are weak because of the variations in the channel weights found across subjects. A stronger interpretation of what brain areas are involved could be found if more subjects were included in the study. Multiple sessions for each subject could also be performed to help control the variation in internal states within each subject. Statistical methods can then be used with the repeated studies to ascertain which channel locations are picked consistently. Channel locations which are used more frequently would then give a stronger sense of which brain areas are involved with finger movements. Observing which lags are used most often for each channel location can also give a stronger sense of the temporal order of when each brain area is active, yielding a framework for the neural network involved with finger movements.

5. Conclusion

In conclusion, we find that EEG signals can be used with a linear decoder with memory to predict the trajectories of repetitive finger movements with fair decoding accuracies that are comparable to those from invasive neural interfaces. However, gathering how the finger tapping task is represented in the brain yielded inconsistent results across subjects, making the interpreted neural representations uncertain. The conviction behind the neural representations would have been stronger if the distributions in the channel weights were similar between subjects.

Appendix

IRB Approval letter

Renewal Application Approval

To: Principal Investigator, Dr. Jose L. Contreras-Vidal, Kinesiology
Student, Trent Jason Bradberry, Kinesiology
Student, Harsha Agashe, Kinesiology
From: James M. Hagberg
IRB Co-Chair
University of Maryland College Park
Re: IRB Protocol: 06-0031 - Non-invasive neural prosthetics for reaching
Approval Date: January 11, 2011
Expiration Date: January 11, 2012
Application: Renewal
Review Path: Expedited

The University of Maryland, College Park Institutional Review Board (IRB) Office approved your Renewal IRB Application. This transaction was approved in accordance with the University's IRB policies and procedures and 45 CFR 46, the Federal Policy for the Protection of Human Subjects. Please reference the above-cited IRB Protocol number in any future communications with our office regarding this research.

Recruitment/Consent: For research requiring written informed consent, the IRB-approved and stamped informed consent document will be sent via mail. The IRB approval expiration date has been stamped on the informed consent document. Please note that research participants must sign a stamped version of the informed consent form and receive a copy.

Continuing Review: If you intend to continue to collect data from human subjects or to analyze private, identifiable data collected from human subjects, beyond the expiration date of this protocol, you must submit a Renewal Application<http://www.umresearch.umd.edu/IRB/renewal%20app.html> to the IRB Office 45 days prior to the expiration date. If IRB Approval of your protocol expires, all human subject research activities including enrollment of new subjects, data collection and analysis of identifiable, private information must cease until the Renewal Application is approved. If work on the human subject portion of your project is complete and you wish to close the protocol, please submit a Closure Report<http://www.umresearch.umd.edu/IRB/closure%20app.html> to irb@umd.edu<mailto:irb@umd.edu>.

Modifications: Any changes to the approved protocol must be approved by the IRB before the change is implemented, except when a change is necessary to eliminate an

apparent immediate hazard to the subjects. If you would like to modify an approved protocol, please submit an Addendum request<http://www.umresearch.umd.edu/IRB/addendum%20app.html> to the IRB Office.

Unanticipated Problems Involving Risks: You must promptly report any unanticipated problems involving risks to subjects or others to the IRB Manager at 301-405-0678 or jsmith@umresearch.umd.edu<mailto:jsmith@umresearch.umd.edu>

Additional Information: Please contact the IRB Office at 301-405-4212 if you have any IRB-related questions or concerns. Email: irb@umd.edu<mailto:irb@umd.edu>

The UMCP IRB is organized and operated according to guidelines of the United States Office for Human Research Protections and the United States Code of Federal Regulations and operates under Federal Wide Assurance No. FWA00005856.

0101 Lee Building
College Park, MD 20742-5125
TEL 301.405.4212
FAX 301.314.1475
irb@umd.edu<mailto:irb@umd.edu>
http://www.umresearch.umd.edu/IRB

IRB Consent Form

Initials _____ Date _____

CONSENT FORM

Project Title	Non-invasive neural prosthetics for reaching
Why is this research being done?	This is a research project being conducted by José L. Contreras-Vidal, Ph.D., Harshavardhan Agashe, and Rodolphe Gentili, Ph.D., at the University of Maryland, College Park. We are inviting you to participate in this research project because you are a healthy, right-handed adult, a healthy adult who has suffered a disarticulation of at the level of the shoulder, elbow or wrist, or have been diagnosed with Parkinson's Disease (PD). The purpose of this research project is to develop non-invasive neural prosthetics that will improve the quality of life of individuals with impaired movement of their upper limbs due to injury (i.e., amputation) or disease (i.e., PD).
What will I be asked to do?	You will be asked to perform the *checked* procedure in the Cognitive Motor Neuroscience Lab in the Health and Human Performance Building: ☐ Procedure 1: Data Collection You will be asked to do the following during the preparation stage (1 hour): 1. Fill out a form with your personal health information. 2. Have your head fitted with an electroencephalography (EEG) cap with up to 128 hollow sensors. The sensors will be filled with conductive gel to ensure good physical contact with your scalp. 3. Have a reference sensor placed on your ear. 4. Have eye activity recorded with sensors around your right eye. 5. Have your head stabilized with a chin rest to minimize head movement. 6. Have 6 infrared emitting diode (IRED) markers placed on your reaching arm. The marker will be visible only to the camera system used to track the movement of your finger. 7. Wear a data-collection glove. You will be asked to perform either (a) or (b) indicated below: (a) Reaching movements to 8 targets using the following instructions (45 minutes): 1. Press the center target. 2. In your mind, select one of the 8 targets. 3. Reach to your selected target. 4. After you have reached the target, return your hand to the center position. 5. After 20 practice trials, there will be 40 trials per target for a total of 320 trials. 6. You may rest between any trials without negatively affecting the study. (b) Reaching movements to and grasping 8 objects using the following instructions (45 minutes) 1. Start with your arm in the resting position. 2. In your mind, select one of the 8 objects. 3. When the indicator light turns green, reach and grasp the selected object. 4. Return your hand to the resting position. 5. After 20 practice trials, there will be 40 trials per target for a total of 320 trials. 6. You may rest between any trials without negatively affecting the study. You will be paid $20 and may be invited back to perform Procedure 2.

Initials _____ Date _____

Project Title	Non-invasive neural prosthetics for reaching
What will I be asked to do? (continued)	☐ Procedure 2: Testing of Computer Cursor Control by Experienced Subjects You will be asked to do the following during the preparation stage (1 hour): 1. Fill out a form with your personal health information. 2. Have your head fitted with an electroencephalography (EEG) cap with up to 64 hollow sensors. The sensors will be filled with conductive gel to ensure good physical contact with your scalp. 3. Have a reference sensor placed on your ear. 4. Have eye activity recorded with sensors around your right eye. 5. Have your head stabilized with a chin rest to minimize head movement. 6. Have electromyography (EMG) sensors placed on the skin of your arm and shoulder with double-sided adhesive tape. Specifically the sensors will be positioned over two muscles responsible for moving your upper arm (anterior and posterior deltoids) and two muscles responsible for moving your forearm (biceps and triceps). The sensors are used for recording the inadvertent muscle activity you may generate. You will be asked to perform *imagined* reaching movements to 8 targets using the following instructions (45 minutes): 1. Keep your hand and arm stationary throughout the entire experiment. 2. Watch the computer cursor move to the target on the computer screen as you continue to *imagine* reaching to the actual target. 3. If you accidentally acquire the wrong target, verbally say so. 4. Think about your hand being in a center position. 5. Watch the computer cursor move to the center position on the computer screen as you continue to *imagine* reaching to the center position. 6. The task will end when you reach 160 times or 45 minutes elapse, which ever occurs first. 7. You may rest between any trials without negatively affecting the study. You will be paid $10 plus $0.16 for each trial completed in less than 10 seconds for a maximum payment of $20. You may be invited back to perform Procedure 3. ☐ Procedure 3: Testing of Robotic Arm Control by Experienced Subjects You will be asked to do the following during the preparation stage (1 hour): 1. Fill out a form with your personal health information. 2. Have your head fitted with an electroencephalography (EEG) cap with up to 64 hollow sensors. The sensors will be filled with conductive gel to ensure good physical contact with your scalp. 3. Have a reference sensor placed on your ear. 4. Have eye activity recorded with sensors around your right eye. 5. Have your head stabilized with a chin rest to minimize head movement. 6. Have electromyography (EMG) sensors placed on the skin of your arm and shoulder with double-sided adhesive tape. Specifically the sensors will be positioned over two muscles responsible for moving your upper arm (anterior and posterior deltoids) and two muscles responsible for moving your forearm (biceps and triceps). The sensors are used for recording the inadvertent muscle activity you may generate.

Initials _____ Date _____

Project Title	Non-invasive neural prosthetics for reaching
What will I be asked to do? (continued)	You will be asked to perform *imagined* reaching movements to 8 targets using the following instructions (45 minutes): 1. Keep your hand and arm stationary throughout the entire experiment. 2. Watch the robotic arm move to the target as you continue to *imagine* reaching to it. 3. If you accidentally acquire the wrong target, verbally say so. 4. Think about your hand being in a center position. 5. Watch the robotic arm move to the center position as you continue to *imagine* reaching to the center position. 6. The task will end when you reach 160 times or 45 minutes elapse, which ever occurs first. 7. You may rest between any trials without negatively affecting the study. You will be paid $10 plus $0.16 for each trial completed in less than 10 seconds for a maximum payment of $20. ☐ Procedure 4: Testing of Robotic Arm Control by Novice Subjects You will be asked to do the following during the preparation stage (1 hour): 1. Fill out a form with your personal health information. 2. Have your head fitted with an electroencephalography (EEG) cap with 32 to 64 hollow sensors. The sensors will be filled with conductive gel to ensure good physical contact with your scalp. 3. Have a reference sensor placed on your ear. 4. Have eye activity recorded with sensors around your right eye. 5. Have your head stabilized with a chin rest to minimize head movement. 6. Have electromyography (EMG) sensors placed on the skin of your arm and shoulder with double-sided adhesive tape. Specifically the sensors will be positioned over two muscles responsible for moving your upper arm (anterior and posterior deltoids) and two muscles responsible for moving your forearm (biceps and triceps). The sensors are used for recording the inadvertent muscle activity you may generate. You will be asked to perform *imagined* reaching movements to 8 targets using the following instructions (45 minutes): 1. Keep your hand and arm stationary throughout the entire experiment. 2. Watch the robotic arm move to the target as you continue to *imagine* reaching to it. 3. If you accidentally acquire the wrong target, verbally say so. 4. Think about your hand being in a center position. 5. Watch the robotic arm move to the center position as you continue to *imagine* reaching to the center position. 6. The task will end when you reach 160 times or 45 minutes elapse, which ever occurs first. 7. You may rest between any trials without negatively affecting the study. You will be paid $10 plus $0.16 for each trial completed in less than 10 seconds for a maximum payment of $20.

Initials _____ Date _____

Project Title	Non-invasive neural prosthetics for reaching
What about confidentiality?	We will do our best to keep your personal information confidential. To help protect your confidentiality, names will not be identified at any time or linked with the data collected (including data stored electronically). A code will be placed on the survey and other collected data. The data provided will generally be grouped with data provided by others for reporting and presentation. Data collected will be secured in a locked filing cabinet in the Cognitive Motor Neuroscience Lab, in the Health and Human Performance Building. Only the Principal Investigator and his collaborators will have access to this locked file cabinet. If we write a report or article about this research project, your identity will be protected to the maximum extent possible. This research project involves making videotapes of you. The videotapes will only be used by the investigators to confirm your movements if there are issues with the data obtained from the other recording equipment. The videotapes will be secured with the other data as described above. These videotapes will be destroyed when the study concludes. ___ I agree to be videotaped during my participation in this study ___ I do not agree to be videotaped during my participation in this study
What are the risks of this research?	You may experience a mild degree of physical discomfort due to prolonged sitting during the EEG cap preparation time and experiment time and removal of the adhesive securing the hand markers and EMG sensors, mental fatigue due to concentration, and/or physical fatigue in the reaching arm if participating in Procedure 1.
What are the benefits of this research?	You will not personally benefit from this study; however, individuals with impaired upper limb movement will greatly benefit from the proposed research. The ability to manipulate the environment will be restored to the motor-disabled population by the use of the thought-controlled neural prosthetic devices developed from this study.
Do I have to be in this research? May I stop participating at any time?	Your participation in this research is completely voluntary. You may choose not to take part at all. If you decide to participate in this research, you may stop participating at any time. If you decide not to participate in this study or if you stop participating at any time, you will not be penalized or lose any benefits to which you otherwise qualify.
Is any medical treatment available if I am injured?	The University of Maryland does not provide any medical, hospitalization, or other insurance for participants in this research study, nor will the University of Maryland provide any medical treatment or compensation for any injury sustained as a result of participation in this research study, except as required by law.
What if I have questions?	This research is being conducted by José L. Contreras-Vidal, Ph.D., and Harshavardhan Agashe at the University of Maryland, College Park in collaboration with Dr. Trent Bradberry from Metron Scientific Solutions. If you have any questions about the research study itself, please contact José L. Contreras-Vidal at 301-405-2495 or pepeum@umd.edu. If you have questions about your rights as a research subject or wish to report a research-related injury, please contact: **Institutional Review Board Office, University of Maryland, College Park, Maryland, 20742; irb@deans.umd.edu; 301-405-0678** This research has been reviewed according to the University of Maryland, College Park IRB procedures for research involving human subjects.
Statement of Age of Subject and Consent	Your signature indicates that: ☐ you are at least 18 years of age ☐ the research has been explained to you ☐ your questions have been fully answered ☐ you freely and voluntarily choose to participate in this research project
Signature and Date	**NAME OF SUBJECT** | **SIGNATURE OF SUBJECT** | **DATE**

Parameters of the Genetic Algorithm

Population Type	Bit String
Population Size	20
Creation Function	Uniform
Crossover Function	Crossover Scattered
Crossover Fraction	0.5
Elite Count	2
Mutation Function	Uniform
Fitness Value	Median correlation coefficient across 10 folds
Fitness Scaling Function	Rank
Selection Function	Stochastic
Stall Generations	50
Function Tolerance	1*10^-12
Maximum Number of Generations	500

Table 3. Parameters used in the Genetic Algorithm. Parameters and options are relevant to the genetic algorithm functions in MATLAB (MathWorks, Inc., Natick, Massachusetts). Each individual was designed to be a string of logical elements, which indicated which channel from which lag was to be used in the decoding. The fitness value was the median of the correlation coefficients across 10 folds from the cross validation scheme. The genetic algorithm was designed to stop when it reached 500 generations or when the improvement in the population fitness value did not improve by 1*10^-12 over 50 generations.

References

Acharya, S., Fifer, M. S., Benz, H. L., Crone, N. E., & Thakor, N. V. (2010). Electrocorticographic amplitude predicts finger positions during slow grasping motions of the hand. *Journal of neural engineering*, *7*(4), 046002. doi: 10.1088/1741-2560/7/4/046002.

Beisteiner, R., Windischberger, C., Lanzenberger, R., Edward, V., Cunnington, R, Erdler, M., et al. (2001). Finger somatotopy in human motor cortex. *NeuroImage*, *13*(6 Pt 1), 1016-26. doi: 10.1006/nimg.2000.0737.

Bansal, A. K., Vargas-Irwin, C. E., Truccolo, W., & Donoghue, J. P. (2011). Relationships among low-frequency local field potentials, spiking activity, and three-dimensional reach and grasp kinematics in primary motor and ventral premotor cortices. *Journal of neurophysiology*, *105*(4), 1603-19. doi: 10.1152/jn.00532.2010.

Bortoletto, M., Cook, A., & Cunnington, Ross. (2011). Motor timing and the preparation for sequential actions. *Brain and cognition*, *75*(2), 196-204. Elsevier Inc. doi: 10.1016/j.bandc.2010.11.016.

Bradberry, T. J., Gentili, R. J., & Contreras-Vidal, J. L. (2010). Reconstructing three-dimensional hand movements from noninvasive electroencephalographic signals. *The Journal of neuroscience : the official journal of the Society for Neuroscience*, *30*(9), 3432-7. doi: 10.1523/JNEUROSCI.6107-09.2010.

Gallivan, J. P., McLean, D. A., Valyear, K. F., Pettypiece, C. E., & Culham, J. C. (2011). Decoding action intentions from preparatory brain activity in human parieto-frontal networks. *The Journal of neuroscience : the official journal of the Society for Neuroscience*, *31*(26), 9599-610. doi: 10.1523/JNEUROSCI.0080-11.2011.

Gerloff, C., Richard, J., Hadley, J., Schulman, a E., Honda, M., & Hallett, M. (1998). Functional coupling and regional activation of human cortical motor areas during simple, internally paced and externally paced finger movements. *Brain : a journal of neurology*, *121 (Pt 8)*, 1513-31. Retrieved from http://www.ncbi.nlm.nih.gov/pubmed/9712013.

Hamed, S. B., Schieber, M H, & Pouget, a. (2007). Decoding M1 neurons during multiple finger movements. *Journal of neurophysiology*, *98*(1), 327-33. doi: 10.1152/jn.00760.2006.

Haupt, R. L. & Haupt, S. E. (2004). *Practical Genetic Algorithms* (2nd ed.). Hoboken, NY: John Wiley & Sons.

Hochberg, L. R., Serruya, M. D., Friehs, G. M., Mukand, J. a, Saleh, M., Caplan, A. H., et al. (2006). Neuronal ensemble control of prosthetic devices by a human with tetraplegia. *Nature*, *442*(7099), 164-71. doi: 10.1038/nature04970.

Indovina, I., & Sanes, J. N. (2001). On somatotopic representation centers for finger movements in human primary motor cortex and supplementary motor area. *NeuroImage*, *13*(6 Pt 1), 1027-34. doi: 10.1006/nimg.2001.0776.

Kubánek, J., Miller, K. J., Ojemann, J G, Wolpaw, J R, & Schalk, G. (2009). Decoding flexion of individual fingers using electrocorticographic signals in humans. *Journal of neural engineering*, *6*(6), 066001. doi: 10.1088/1741-2560/6/6/066001.

Leuthardt, E. C., Schalk, Gerwin, Wolpaw, Jonathan R, Ojemann, Jeffrey G, & Moran, D. W. (2004). A brain-computer interface using electrocorticographic signals in humans. *Journal of neural engineering*, *1*(2), 63-71. doi: 10.1088/1741-2560/1/2/001.

Pfurtscheller, G., & Lopes da Silva, F. H. (1999). Event-related EEG/MEG synchronization and desynchronization: basic principles. *Clinical neurophysiology : official journal of the International Federation of Clinical Neurophysiology*, *110*(11), 1842-57. Retrieved from http://www.ncbi.nlm.nih.gov/pubmed/10576479.

Pfurtscheller, G., Zalaudek, K., & Neuper, C. (1998). Event-related beta synchronization after wrist, finger and thumb movement. *Electroencephalography and clinical neurophysiology*, *109*(2), 154-60. Retrieved from http://www.ncbi.nlm.nih.gov/pubmed/9741806.

Schieber, Marc H, & Santello, M. (2004). Hand function: peripheral and central constraints on performance. *Journal of applied physiology (Bethesda, Md. : 1985)*, *96*(6), 2293-300. doi: 10.1152/japplphysiol.01063.2003.

Toni, I., Schluter, N. D., Josephs, O., Friston, K., & Passingham, R. E. (1999). Activity in the Human Brain : An Event-related fMRI Study. *Cerebral Cortex*, 35-49.

Vargas-Irwin, C. E., Shakhnarovich, G., Yadollahpour, P., Mislow, J. M. K., Black, M. J., & Donoghue, J. P. (2010). Decoding complete reach and grasp actions from local primary motor cortex populations. *The Journal of neuroscience : the official journal of the Society for Neuroscience*, *30*(29), 9659-69. doi: 10.1523/JNEUROSCI.5443-09.2010.

Wildgruber, D., Erb, M., Klose, U., & Grodd, W. (1997). Sequential activation of supplementary motor area and primary motor cortex during self-paced finger movement in human evaluated by functional MRI. *Neuroscience letters*, *227*(3), 161-4. Retrieved from http://www.ncbi.nlm.nih.gov/pubmed/9185675.

Yuan, H., Perdoni, C., & He, B. (2010). Relationship between speed and EEG activity during imagined and executed hand movements. *Journal of neural engineering*, *7*(2), 26001. doi: 10.1088/1741-2560/7/2/026001.

Zhuang, J., Truccolo, W., Vargas-Irwin, C., & Donoghue, J. P. (2010). Decoding 3-D reach and grasp kinematics from high-frequency local field potentials in primate primary motor cortex. *IEEE transactions on bio-medical engineering*, *57*(7), 1774-84. doi: 10.1109/TBME.2010.2047015.